

## ARTICLE

**First Principle Study on the Magnetic and Electric Properties of Wurtzite Cr-phosphides and Cr-sulphides: Several Half-metallic Ferromagnets**Jun Liu<sup>a\*</sup>, Pei-da Chen<sup>a</sup>, Li Chen<sup>a</sup>, Hui-ning Dong<sup>a</sup>, Rui-lun Zheng<sup>b</sup>*a. Institute of Applied Physics, and College of Mathematics and Physics, Chongqing University of Posts and Telecommunications, Chongqing 400065, China**b. School of Physical Science and Technology, Southwest University, Chongqing 400715, China*

(Dated: Received on September 2, 2009; Accepted on June 12, 2010)

The geometrical structures of wurtzite CrX (X=As, Sb, O, Se, and Te) were optimized, then their electric and magnetic properties were investigated by the first-principle calculations within the generalized gradient approximation for the exchange-correlation functional based on the density functional theory. These Cr-phosphides and Cr-sulphides were predicted to be half-metallic ferromagnets whose spin-polarization at the Fermi level is absolutely 100%. The molecular magnetic moments of Cr-phosphides and Cr-sulphides are 3.00 and 4.00  $\mu_B$ , which arise mainly from Cr-ions, respectively. There is ferromagnetic coupling in both Cr-phosphides and Cr-sulphides. The Curie temperatures of Cr-sulphides and Cr-phosphides are high. The electronic structures of Cr-ions are  $a_{1g}^2 \uparrow \downarrow t_{1u}^4 \uparrow \downarrow t_{1u}^1 \uparrow e_g^2 \uparrow$  in Cr-phosphides and  $a_{1g}^2 \uparrow \downarrow t_{1u}^4 \uparrow \downarrow t_{1u}^1 \uparrow t_{2g}^3 \uparrow$  in Cr-sulphides, respectively.

**Key words:** Half-metallic ferromagnet, Electric and magnetic property, Molecular magnetic moment

**I. INTRODUCTION**

Spintronics, which exploit the spins of electrons as well as their charges, have promising application prospects [1–3]. Many spintronic devices, such as high quality magnetoresistance random access memories (MRAMs), magnetic sensors and read-write magnetic-head of computers will be invented in the near future. For spintronic applications, materials having large molecular magnetic moments and high Curie temperatures are critical [4]. The transition-metal or rare-earth element doped semiconductors and diluted magnetic semiconductors (DMSs) both have large molecular magnetic moments. However, their Curie temperatures are not high enough for their applications. For instance, the Curie temperature of Mn-doped GaAs is much lower than the room temperature [4–6]. The half-metallic ferromagnets (HMFs) have complete spin-polarization, which is theoretically  $\pm 100\%$  at the Fermi level [7–9]. This means that one spin channel is metallic while the other is insulating in HMFs, which is much different from usual ferromagnetic metals such as iron, nickel, cobalt, and their alloys. Layered structures incorporated from HMFs can possibly exhibit large magnetoresistance, and so show great promise for a variety of valuable devices such as MRAMs, spin transistors, and spin diodes.

The Curie temperatures of HMFs are often higher than those of magnetic semiconductors possibly. The Curie temperatures of zinc blende (ZB) CrAs and spinel  $Fe_3O_4$  are 400 and 858 K, respectively, which are higher than the room temperature [2, 10–12]. Furthermore, the resistivity of HMFs matches well with that of semiconductors, so they are the best electrode materials from which the completely spin-polarized electrons are transmitted into the DMSs. Therefore, HMFs have attracted much attention in the past few years. Recently, much attention has been paid to transition-metal doped or pure zinc blende semiconductor-type HMFs. Many hypothetical ZB materials such as CrAs, CrSb, GaAs, GaSb, CrP, MnC, MnSb, and doped ZnTe had been predicted to have half-metallicity from the theoretical calculations [10, 13–17].

Other hypothetical materials such as spinel  $Fe_3O_4$  and  $NiFe_2O_4$ , rutile  $CrO_2$  had also been predicted to have half-metallicity [11, 12, 18–20]. Some of these hypothetical HMFs had been prepared and found to have half-metallicity experimentally [10–20]. However, there is little attention paid to wurtzite HMFs.

In this work, some wurtzite HMFs were predicted and their magnetic and electric properties were investigated in detail based on the density functional theory.

**II. TECHNICALITY**

The geometrical structures of hypothetical wurtzite supercells of CrX (X=As, Sb, O, Se, and Te) including two cations and two anions were optimized. Their space groups are P1. During the optimization, the su-

\* Author to whom correspondence should be addressed. E-mail: liujun@cqupt.edu.cn

percell lattice constants were adjusted based on the variation of their energy by the software until the energy convergence was less than  $2 \mu\text{eV}/\text{atom}$ . The optimizations and calculations were performed using the calculation module “castep” of the software “materials studio” based on the density functional theory. The optimization quality “fine” was selected, corresponding to the cutoff energy 340 eV and the  $k$ -point set  $9 \times 4 \times 5$ . The magnetic and electric properties were calculated by LDA+U method. The calculation quality was selected as “fine”, corresponding to the cutoff energy 310 eV and the  $k$ -point set  $7 \times 7 \times 4$ . The wave functions are expanded with plane-wave pseudo-potentials, and the exchange correlation functions are the Perdew-Burke-Ernzerh functions (PBE) of three nonlocal gradient-corrected exchange-correlation functions (GGA). The calculated electronic structures of isolated atoms include  $\text{Cr}3s^23p^63d^54s^1$ ,  $\text{As}4s^24p^3$ ,  $\text{Sb}5s^25p^3$ ,  $\text{O}2s^22p^4$ ,  $\text{Se}4s^24p^4$ , and  $\text{Te}5s^25p^4$ .

The lattice parameters of wurtzite ZnO, CrAs, and CrTe were calculated and compared with experimental or calculated results of others in order to confirm our calculations [21–26]. Other parameters of CrX including the  $E_g$ ,  $E_h$ , and  $M$  were also calculated [21–26]. Here, the  $E_g$  indicates the spin energy gaps, defined as the energy distance from the maximum energy of spin-down valence subbands to the minimum energy of the spin-down conductive subbands. The  $E_h$  indicates the spin-flip gaps or half-metallic gaps, defined as the minimum of  $E_v$  and  $E_c$ , where  $E_v$  and  $E_c$  show the energy distances from the valence band peak and the conductive band bottom of semiconductor subbands to the Fermi level of conductive subbands, respectively. The  $M$  indicates the supercell magnetic moments. All calculated parameters were shown in Table I. From Table I, our calculated lattice constants of CrAs ( $a=4.03 \text{ \AA}$ ,  $b=8.06 \text{ \AA}$ , and  $c=6.55 \text{ \AA}$ ) and CrTe ( $a=4.47 \text{ \AA}$ ,  $b=8.94 \text{ \AA}$ , and  $c=7.29 \text{ \AA}$ ) accord well with those calculated by Xie and Zhang, respectively [10, 24, 25]. Furthermore, the calculated lattice constants of ZnO ( $a=3.29 \text{ \AA}$ ,  $b=6.58 \text{ \AA}$ , and  $c=5.31 \text{ \AA}$ ) also ac-

cord well with the experimental values in Ref.[26]. This means that our calculations are reliable.

From Table I, The lattice constants  $a$  and  $c$  of Cr-phosphides and Cr-sulphides grow larger with the increasing of the principle quantum numbers of the anions. The main reason is that the radius of isolated atoms grows larger with the increasing of the principle quantum numbers of the anions. On the other hand,  $c/a$  of Cr-sulphides is evidently larger than those of Cr-phosphides totally. The main reason is that the sulfur family elements have one electron more than Nitrogen family elements if their principle quantum numbers are same, so there is stronger coulomb repulsion in Cr-sulphide supercells than in Cr-phosphide cells if their volumes are same. Stronger coulomb repulsion will result in huger expansion of these compounds along  $c$ -axis.

### III. RESULTS AND DISCUSSION

#### A. Spin-polarized densities of states and energy bands

The spin-polarized densities of states (DOSs) of wurtzite CrAs and CrSb are shown in Fig.1 (a) and (b), where the curves above and below the line indicating the DOSs=0 show the DOSs of spin-up and spin-down subbands, respectively. The spin-polarized energy bands of wurtzite CrAs and CrSb are shown in Fig.1 (c) and (d), where the solid and dashed curves show the spin-down and spin-up subbands, respectively. From Fig.1, the spin polarization of CrAs and CrSb are both 100% since they both have only spin-up subbands at the Fermi level. This means that the spin-up subbands are conductive, but the spin-down subbands are semiconductive. Furthermore, from Table I their molecular magnetic moments are both integral number, namely  $3.00 \mu_B$ . Having integral magnetic moments is one of important characters of HMFs. This means that they are potentially half-metallic ferromagnets and they have high enough molecular magnetic moments. Comparing Fig.1 with Table I, the  $E_g$  of CrAs and CrSb are about 4.00 and 2.86 eV, respectively. This means that CrAs and CrSb potentially have high Curie temperatures since the Curie temperatures of magnetic materials increase with their  $E_g$  generally [10–12]. Based on the above analysis, wurtzite CrAs and CrSb have more promising application prospects than diluted magnetic semiconductors in spintronics.

On the other hand, the spin-up and spin-down TDOSs of CrAs and CrSb are both divided into five parts. Their TDOSs are similar when their energy is lower than  $-9.1 \text{ eV}$ . The TDOSs below  $-9.1 \text{ eV}$  are not plotted in Fig.1 confined by the sizes of these figures. The reason is mainly that isolated As- and Sb-atoms have similar outer orbital structures including their  $ns$  and  $np$  orbits. The first part with energy from  $-74.2 \text{ eV}$  to  $-66.4 \text{ eV}$  comes from  $3s$  orbits of cations. The second part with energy from  $-45.3 \text{ eV}$  to  $-38.1 \text{ eV}$  comes from  $3p$  orbits of cations. The third part with energy from  $-13.0 \text{ eV}$  to  $-9.1 \text{ eV}$  comes from  $ns$  or-

TABLE I Calculated or experimental lattice constants,  $E_g$ ,  $E_h$ , and  $M$  of several wurtzite materials.

Compounds	$a/\text{\AA}$	$b/\text{\AA}$	$c/\text{\AA}$	$E_g/\text{eV}$	$E_h/\text{eV}$	$M/\mu_B$
CrAs	4.03	8.06	6.55	4.00	0.50	3.00
CrAs [10]	4.00	8.00	6.53			
CrSb	4.40	8.80	6.90	2.86	0.06	3.00
CrO	3.29	7.58	5.67	5.01	0.50	4.00
CrSe	4.12	8.24	6.86	4.69	2.28	4.00
CrTe	4.47	8.94	7.25	4.23	1.41	4.00
CrTe [10, 24]	4.46	8.92	7.23			
ZnO	3.29	7.58	5.31			
ZnO [25]	3.28	7.56	5.32			
ZnO [26]	3.25	7.50	5.32			

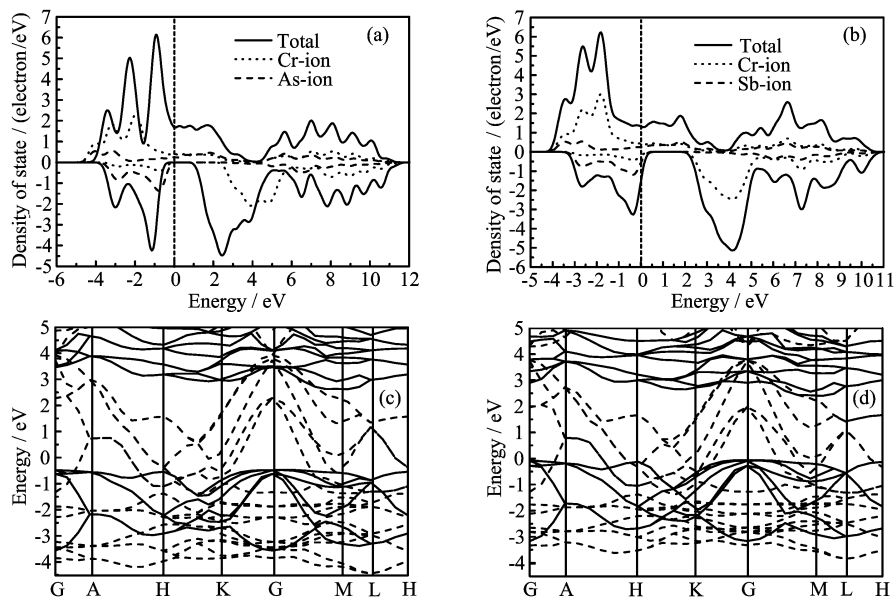


FIG. 1 Spin-polarized state densities of CrAs and CrSb shown in (a) and (b) respectively. Spin-polarized energy bands of CrAs and CrSb shown in (c) and (d) (dashed lines are up-spin, solid lines are down-spin), respectively.

bits of anions. The spin-up and spin-down subbands below  $-9.1$  eV are symmetrical with the line showing  $\text{DOS}=0$ , and their energy is far lower than the Fermi level. Therefore, these orbits are localized in their ions and can cause no influence on the magnetic and electric properties of Cr-phosphides. The fourth spin-up part goes through the Fermi level, so they cause main contribution on the conductivity of Cr-phosphides. However, the fourth spin-down part lies below the Fermi level and it is asymmetrical with the spin-up part, so the fourth part causes main influence on the magnetic properties of Cr-phosphides. They come mainly from 3d orbits of cations and  $np$  orbits of anions, and partly from 4s orbits of cations from Fig.1 (a) and (b). This shows that there are hybridized orbits from d, p, and s orbits in Cr-phosphides.

Spin-polarized TDOSs and LDOSs of wurtzite  $\text{CrX}$  ( $X=\text{O}, \text{Se}, \text{and Te}$ ) are shown in Fig.2 (a), (b), and (c), respectively. Here, the solid curves show their TDOSs, and the dots and the dashed curves show the LDOSs of one Cr-ion and one X-ion ( $X=\text{O}, \text{Se}, \text{and Te}$ ), respectively. Spin-polarized energy bands of  $\text{CrX}$  ( $X=\text{O}, \text{Se}, \text{and Te}$ ) are shown in Fig.2 (d), (e), and (f), respectively. Here, the solid and dashed curves show the spin-down and spin-up subbands, respectively. From Fig.2, there are only spin-up subbands at the Fermi level, so the spin polarization of these Cr-sulphides is all 100%. Furthermore, from Table I their molecular magnetic moments are all  $4.00 \mu_{\text{B}}$ , which are integral and larger than those of Cr-phosphides. This means that they are potentially half-metallic ferromagnets. Comparing Fig.2 with Table I, the  $E_{\text{g}}$  of CrO, CrSe, and CrTe are about 5.01, 4.69, and 4.23 eV, respectively. This means that Cr-sulphides possibly have larger  $E_{\text{g}}$ ,

and then higher Curie temperatures than Cr-phosphide. Furthermore, the  $E_{\text{h}}$  of Cr-sulphides are possibly larger than those of Cr-phosphides from Table I. This indicates that the half-metallicity of Cr-sulphides is more stable than that of Cr-phosphides possibly.

The TDOSs of Cr-sulphides are also divided into five parts. They are similar to those of Cr-phosphides when their energy is lower than  $-9.1$  eV. However, the  $E_{\text{g}}$  and  $E_{\text{h}}$  of Cr-sulphides are larger than those of Cr-phosphides. This means that there is stronger crystal field in Cr-sulphides than that in Cr-phosphides. The reason is mainly that one anion of Cr-sulphides has one electron more than one anion of Cr-phosphides correspondingly. The first, the second, and the third part come from Cr 3s-orbits, Cr 3p-orbits, and  $ns$ -orbits of anions, respectively. The spin-up and spin-down subbands of these three parts are axially symmetrical and localized in their ions, so they can cause no influence on the magnetic and electric properties of Cr-sulphides. The fourth part comes from the hybridization of 3d- and 4s-orbits of cations and  $np$ -orbits of anions. The fourth part can cause important influence on the magnetic and electric properties of Cr-sulphides

From Fig.1 and Fig.2, both Cr-phosphides and Cr-sulphides are conductive by spin-up transmitted electrons. However, their spin-up subbands through the Fermi level are narrower than those of usual ferromagnetic metals or their alloys. This means that their conductivity is much lower than that of usual ferromagnetic metals or their alloys. Therefore, Cr-phosphides and Cr-sulphides are possibly better electrode materials of diluted magnetic semiconductors than usual ferromagnetic metals or their alloys since their conductivity accords with that of semiconductors.

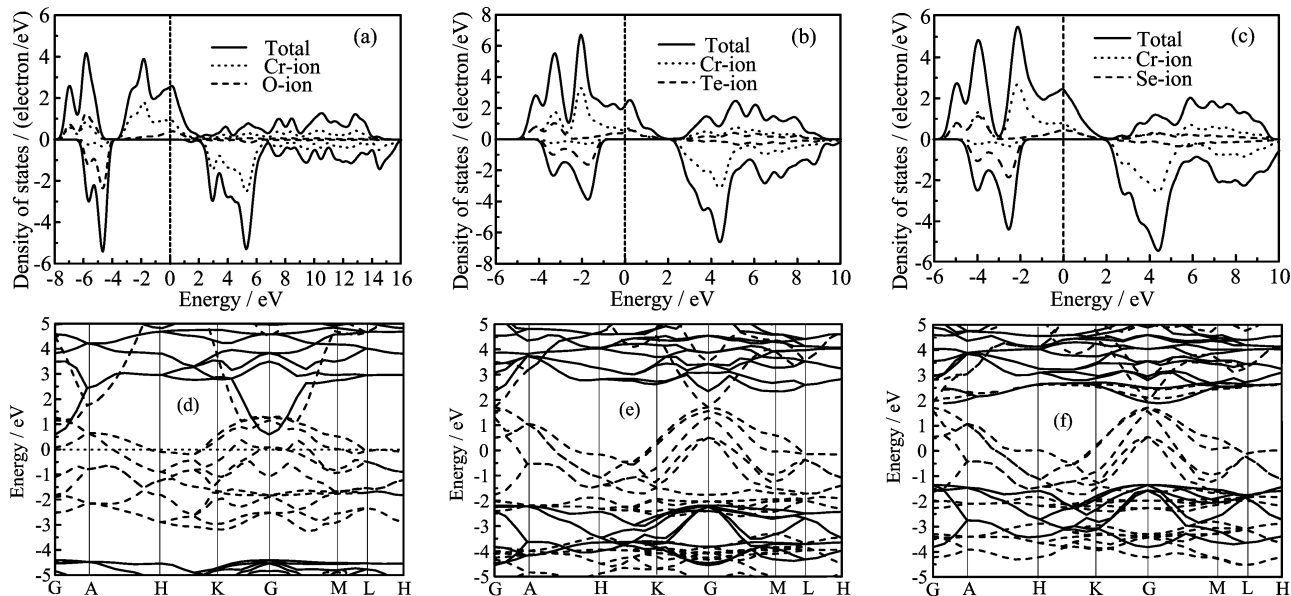


FIG. 2 Spin-polarized state densities of CrO, CrSe, and CrTe shown in (a), (b), and (c), respectively. Spin-polarized energy bands of CrO, CrSe, and CrTe shown in (d), (e), and (f) (dashed lines are spin-up, solid lines are spin-down), respectively.

TABLE II Ionic parameters of some wurtzite Cr-phosphides and Cr-sulphides including the number of s, p, d, and total electrons ( $N_s$ ,  $N_p$ ,  $N_d$ , and  $N_t$ ), the charges  $Q$  and the ionic magnetic moments  $M_i$ .

Compound	Ion	$N_s$	$N_p$	$N_d$	$N_t$	$Q$	$M_i/\mu_B$
CrAs	Cr	2.72	6.71	4.80	14.22	0.22	4.46
	As	1.23	3.55	0.00	4.78	-0.22	-1.46
CrSb	Cr	2.77	6.74	4.88	14.38	-0.38	4.50
	Sb	1.24	3.37	0.00	4.62	0.38	-1.50
CrO	Cr	2.30	6.42	4.56	13.31	0.69	4.36
	O	1.87	4.82	0.00	6.69	-0.69	-0.36
CrSe	Cr	2.63	6.75	4.73	14.11	-0.11	4.74
	Se	1.41	4.49	0.00	5.89	0.11	-0.74
CrTe	Cr	2.72	6.85	4.79	14.36	-0.36	4.54
	Te	1.34	4.30	0.00	5.64	0.36	-0.54

## B. Electronic structures of wurtzite Cr-phosphides and Cr-sulphides

The ionic parameters of Cr-phosphide and Cr-sulphide supercells are shown in Table II. There are two cations and two anions in a supercell, but the ionic parameters of only one cation and one anion are given in Table II since two cations or two anions of one compound have the same ionic parameters, respectively. These ionic parameters include the number of s, p, d, and total electrons ( $N_s$ ,  $N_p$ ,  $N_d$ , and  $N_t$ ), the charges  $Q$  and the ionic magnetic moments. From Table II, the ionic magnetic moments of a Cr-ion in CrAs, CrSb, CrO, CrSe, and CrTe are 4.46, 4.50, 4.36, 4.74, and 4.54  $\mu_B$ , respectively. These ionic magnetic moments are proximity. However, the absolute values of the ionic magnetic moments of one As- and Sb-ion are 1.46 and 1.50  $\mu_B$ , which are both evidently larger than 0.36,

0.74, and 0.54  $\mu_B$  of one O-, Se-, and Te-ion, respectively. This means that there are ferromagnetic coupling between the cations and anions in Cr-phosphides and Cr-sulphides, but the ferromagnetic coupling in Cr-phosphides is evidently stronger than that in Cr-sulphides. This results in that the molecular magnetic moments of Cr-sulphides are larger than those of Cr-phosphides. After adding up the ionic magnetic moments we can get the molecular magnetic moments. They are 3.0  $\mu_B$  for Cr-phosphides, but 4.0  $\mu_B$  for Cr-sulphides.

From the ligand field theory [28], there are four anion-ligands around one Cr-ion. The Cr-ion and its ligands form the coordinate compound  $ML_4$ . There is strong tetrahedral crystal field in  $ML_4$ , which results in Cr 3d-orbits being split into bonding orbits containing two  $e_g$ -orbits and three  $t_{2g}$  orbits with lower energy, and their corresponding anti-bonding orbits containing two

$e_g^*$  and three  $t_{2g}^*$  orbitals with higher energy. Generally, the energy of the  $e_g$  orbitals is lower than that of the  $t_{2g}$  orbitals. However, the energy of the  $t_{2g}$  orbitals is possibly lower than that of  $e_g$  orbitals if the crystal field is strong enough in order to decrease the energy of the compounds. Therefore, the energy of the  $t_{2g}$  orbitals is possibly lower than that of  $e_g$ -orbitals in Cr-sulphides. The Cr3d orbitals will hybrid with Cr4s orbitals and  $np$ -orbitals of anions because their energy is near to each other. These hybridized orbitals are split into one  $t_{1g}$ , three  $t_{1u}$ , two  $e_g$ , and three  $t_{3g}$  orbitals. The energy of  $t_{1g}$  and  $t_{1u}$  orbitals is much lower than that of  $e_g$  and  $t_{3g}$  in both Cr-phosphides and Cr-sulphides. On the other hand, the energy difference between  $t_{1g}$ ,  $t_{1u}$ , and  $e_g$  orbitals is much lower than that between  $t_{2g}$  and  $e_g$  in Cr-phosphides. Similarly, the energy difference between  $t_{1g}$ ,  $t_{1u}$ , and  $t_{2g}$  orbitals is much lower than that between  $t_{2g}$  and  $e_g$  orbitals in Cr-sulphides. From the structures of isolated atoms, there are nine electrons containing five Cr3d electrons, one Cr4s electron and three  $np$ -electrons of anions to enter into the molecular orbitals of Cr-phosphides. There are ten electrons to enter into the molecular orbitals of Cr-sulphide. Therefore, the electronic structures of Cr-ions are  $Cr a_{1g}^2 \uparrow \downarrow t_{1u}^4 \uparrow \downarrow t_{1u}^1 \uparrow e_g^2 \uparrow$  in Cr-phosphides and  $a_{1g}^2 \uparrow \downarrow t_{1u}^4 \uparrow \downarrow t_{1u}^1 \uparrow t_{2g}^3 \uparrow$  in Cr-phosphides, respectively, based on the lowest energy principle. From the electronic structures, the molecular magnetic moments of Cr-phosphides and Cr-sulphides are 3.00 and 4.00  $\mu_B$ , respectively. They accord with those given in Table II.

#### IV. CONCLUSION

We have explored the structural, electronic and magnetic properties of wurtzite CrX (X=As, Sb, O, Se, and Te) by performing the first-principle calculations within the GGA-PBE for the exchange-correlation functional. Wurtzite CrX are predicted to be half-metallic ferromagnets, whose spin-polarization at the Fermi level is absolute 100%. The molecular magnetic moments of Cr-phosphides and Cr-sulphides are 3.00 and 4.00  $\mu_B$ , respectively. The ferromagnetic coupling between the cations and anions in Cr-phosphides is evidently stronger than that in Cr-sulphides. The half-metallic gaps, and then the Curie temperatures of Cr-sulphides are higher than those of Cr-phosphides. The electronic structures of Cr-ions are  $a_{1g}^2 \uparrow \downarrow t_{1u}^4 \uparrow \downarrow t_{1u}^1 \uparrow e_g^2 \uparrow$  in Cr-phosphides and  $a_{1g}^2 \uparrow \downarrow t_{1u}^4 \uparrow \downarrow t_{1u}^1 \uparrow t_{2g}^3 \uparrow$  in Cr-sulphides, respectively.

#### V. ACKNOWLEDGMENTS

This work was supported by the Chongqing Natural Science Foundation (No.CSTC2007BB4391 and No.CSTC2008BB4083) and the Chongqing Science and Technology Foundation (No.kj060515 and No.kj080518).

- [1] J. W. Cai, Prog. Phys. **26**, 180 (2006).
- [2] S. K. Ren, F. M. Zhang, and Y. W. Du, Prog. Phys. **24**, 381 (2004).
- [3] J. Cibert, J. F. Bobo, and U. Luders, Comp. Rend. Phys. **6**, 977 (2005).
- [4] J. E. Pask, L. H. Yang, C. Y. Fong, W. E. Pickett, and S. Dag, Phys. Rev. B **67**, 224420 (2003).
- [5] Y. Shen, J. Q. Wang, H. Z. Xing, J. G. Yu, H. B. Mao, and B. Lv, J. Magn. Magn. Mater. **313**, 17 (2007).
- [6] B. Lv, J. Q. Wang, J. G. Yu, H. B. Mao, S. Ye, Z. Q. Zhu, and H. Z. Xing, Appl. Phys. Lett. **90**, 142513 (2007).
- [7] R. A. de Groot, F. M. Mueller, P. G. Van Engen, and K. H. J. Buschow, Phys. Rev. Lett. **50**, 2024 (1983).
- [8] B. Hackenbroich, H. Zare-Kolsaraki, and H. Micklitz, Appl. Phys. Lett. **81**, 514 (2002).
- [9] M. Kopcewicz, F. Stobiecki, J. Jagielski, B. Szymanski, M. Urbaniak, and T. Lucinski, J. Magn. Magn. Mater. **286**, 437 (2005).
- [10] W. H. Xie and B. G. Liu, J. Appl. Phys. **96**, 3559 (2004).
- [11] J. Liu, X. M. Chen, Y. Liu, and H. N. Dong, Sol. Stat. Ion. **179**, 881 (2008).
- [12] J. Liu, X. Q. Wang, Y. Liu, and H. N. Dong, Chin. J. Chem. Phys. **20**, 291 (2007).
- [13] X. F. Ge and Y. M. Zhang, J. Magn. Magn. Mater. **321**, 198 (2009).
- [14] Y. Asano, Y. Tanaka, and A. A. Golubov, Phys. Rev. Lett. **98**, 07002 (2007).
- [15] X. G. Wan, M. Kohno, and X. Hu, Phys. Rev. Lett. **95**, 146602 (2005).
- [16] Y. H. A. Wang, A. Gupta, M. Chshiev, and W. H. Butler, Appl. Phys. Lett. **92**, 062507 (2008).
- [17] M. Ferhat, A. Zaoui, and R. Ahuja, Appl. Phys. Lett. **94**, 142502 (2009).
- [18] X. G. Xu, C. Z. Wang, W. Liu, X. Meng, Y. Sun, and G. Chen, Acta. Phys. Sin. **54**, 313 (2005).
- [19] C. M. Aerts, P. Strange, M. Horne, W. M. Temmerman, Z. Szotek, and A. Svane, Phys. Rev. B **69**, 045115 (2004).
- [20] Z. Szotek, W. M. Temmerman, A. Svane, L. Petit, G. M. Stocks, and H. Winter, Phys. Rev. B **68**, 054415 (2003).
- [21] L. H. Ye, A. J. Freeman, and B. Delley, Phys. Rev. B **73**, 033203 (2006).
- [22] G. Y. Gao, K. L. Yao, E. Şaşıoğlu, L. M. Sandratskii, Z. L. Liu, and J. L. Jiang, Phys. Rev. B **75**, 174442 (2007).
- [23] H. Q. Sun, S. F. Ding, Y. T. Wang, B. Deng, and G. H. Fan, Acta Phys. Chim. Sin. **24**, 1233 (2008).
- [24] M. Zhang, E. Brück, F. R. de Boer, and G. H. Wu, J. Appl. Phys. **97**, 10C306 (2005).
- [25] R. Q. Wu, G. W. Peng, L. Liu, and Y. P. Feng, Appl. Phys. Lett. **89**, 082504 (2006).
- [26] Y. N. Xu and W. Y. Ching, Phys. Rev. B **48**, 4335 (1993).
- [27] R. D. Vispute, V. Talyansky, and S. Choopun, Appl. Phys. Lett. **73**, 34 (1998).
- [28] G. D. Zhou and L. Y. Duan, *Structural Chemistry*, Beijing: Peking University Press, (2004).